

Toward the Wave Digital Real-Time Emulation of Audio Circuits with Multiple Nonlinearities

1st Alessandro Proverbio, 2nd Alberto Bernardini, 3rd Augusto Sarti

Dipartimento di Elettronica, Informazione e Bioingegneria (DEIB), Politecnico di Milano,

Piazza Leonardo Da Vinci 32, 20133 Milano, Italy

alessandro1.proverbio@mail.polimi.it, alberto.bernardini@polimi.it, augusto.sarti@polimi.it

Abstract—Over the past two decades, Wave Digital Filters have been extensively used in the fields of sound synthesis through physical modeling and Virtual Analog modeling to emulate audio circuits in an efficient and modular fashion. However, as far as the implementation of circuits with multiple nonlinearities is concerned, much research effort is still needed in order to develop systematic strategies for solving the corresponding multivariate systems of implicit equations with low computational requirements. In this regard, this paper discusses the computational cost of the Scattering Iterative Method (SIM), a recently proposed iterative fixed-point algorithm that works in the Wave Digital domain and it is capable of handling circuits with J one-port nonlinearities using J separate local solvers. In the light of the computational cost analysis, we also propose a refinement of SIM relying on the so called Dynamic Scattering Matrix Recomputation (DSR) procedure. The DSR procedure significantly improves the performance of the algorithm, paving the way toward Virtual Analog applications in which SIM-based audio plugins emulating nonlinear circuits run in real-time.

Index Terms—Digital Audio Signal Processing, Nonlinear Audio Circuits, Virtual Analog Modeling, Wave Digital Filters

I. INTRODUCTION

Over the past two decades, Wave Digital Filters (WDFs) have been extensively used in the fields of sound synthesis through physical modeling and Virtual Analog modeling to emulate audio circuits in an efficient and modular fashion [1], [2]. WDF theory, introduced by A. Fettweis [3], provides us with a systematic methodology for building digital models of analog circuits through the discretization of their individual components. Wave Digital (WD) structures can be directly derived from the circuit schematic, creating an input-output block for each element in the circuit and then connecting the blocks through topological junctions [4]–[8]. Dynamic circuits with up to one nonlinear element can be implemented using only *explicit* relations and with no need of iterative solvers to run [9]–[15]. This is a considerable advantage of WD modeling over Virtual Analog modeling methods that work in the Kirchhoff domain, as they are typically characterized by sets of implicit equations and involve the use of iterative methods. This benefit, however, does not apply to circuits with multiple nonlinearities, that are unavoidably described by implicit equations [16]. Even in these cases, however, working in the WD domain has proven beneficial. Mainstream strategies that work in the Kirchhoff domain, like Spice-like software based on the Modified Nodal Analysis [17], State-Space methods [18] or Port-Hamiltonian methods

[19], require the use of multi-dimensional iterative solvers (e.g., Newton-Raphson) based on large Jacobian matrices for solving multivariate nonlinear systems of implicit equations. The size of these systems of equations is typically in the order of the number of nodes or the number of meshes of the reference circuit and the same is the size of the Jacobian matrices to be inverted. In the WD domain, instead, especially thanks to the possibility of modeling the topological junctions separately from the elements of the reference circuit, less computationally-demanding methods are available. Reference [20] proposes a WD method that handles circuits with J nonlinear elements using a J -dimensional Newton-Raphson (NR) solver, exploiting the separability of the nonlinear part of the circuit from the linear one. This is a noticeable improvement with respect to the aforementioned methods in the Kirchhoff domain, because the involved Jacobian matrices are smaller, since their size is proportional to the number of nonlinear elements only, and not to the overall number of elements. An alternative fixed-point iterative technique for accommodating multiple nonlinearities in the WD domain that invokes the multi-dimensional WDF paradigm is proposed in [21], [22]. In this paper, we consider another fixed-point iterative method that also operates in the WD domain, called Scattering Iterative Method (SIM). SIM has proven capable of solving photovoltaic networks with thousands of nonlinear elements far more efficiently than Spice-like software [23], [24] and has already demonstrated its potential in Virtual Analog modeling applications [25], [26] showing to be comparable to state-of-the-art techniques in terms of computational cost [25]. The main difference between SIM and WD techniques based on multi-dimensional Jacobian matrices [20] is that, dealing with J one-port nonlinearities, SIM requires J one-dimensional solvers instead of one J -dimensional NR solver. This fact implies greater robustness, guaranteed convergence when working with monotonically increasing i - v nonlinearities (such as diodes), greater efficiency and the possibility of solving the nonlinearities in a parallel fashion with separate threads of execution. SIM has also several features that differentiate it from the fixed-point methods proposed in [21], [22]; in fact, SIM is not formalized by invoking the multi-dimensional WDF framework, the topology is modeled by a single multi-port junction and, more importantly, the free parameters (one per port) introduced in the WD domain are tuned in such a way that they match specific optimal values as much as possible,

in order to speed up convergence.

In this paper we will provide an in-depth analysis of the computational requirements of SIM. In the light of this, we will propose a technique, called *Dynamic Scattering Matrix Recomputation*, to increase its performance. As an example of application, we will present a WD implementation of an asymmetric diode clipper with five diodes (each one accommodated as a separated nonlinearity) that runs in real-time both in the MATLAB environment and in a C++ audio plugin.

II. BACKGROUND ON WORKING PRINCIPLES OF SIM

In the WD domain circuit elements and topological junctions are modeled as separated input-output blocks characterized by scattering relations and related by port connections [3]. Let us consider the class of circuits modeled in the WD domain using $N > 1$ one-port elements connected to one N -port topological junction. We also assume that the first J one-ports with $J < N$ are nonlinear. Given the vector of port voltages across the elements $\mathbf{v} = [v_1, \dots, v_N]^T$ and the vector of port currents through the elements $\mathbf{i} = [i_1, \dots, i_N]^T$, WD variables are defined as

$$\mathbf{a} = \mathbf{v} + \mathbf{Z}\mathbf{i} \quad , \quad \mathbf{b} = \mathbf{v} - \mathbf{Z}\mathbf{i} \quad , \quad (1)$$

where $\mathbf{a} = [a_1, \dots, a_N]^T$ is the vector of voltage waves incident to the elements and reflected from the junction, $\mathbf{b} = [b_1, \dots, b_N]^T$ is the vector of voltage waves reflected from the elements and incident to the junction, $\mathbf{Z} = \text{diag}[Z_1, \dots, Z_N]$ is a diagonal matrix of scalar non-zero free parameters called *port resistances*. The inverse mapping of (1) is

$$\mathbf{v} = \frac{1}{2}(\mathbf{a} + \mathbf{b}) \quad , \quad \mathbf{i} = \frac{1}{2}\mathbf{Z}^{-1}(\mathbf{a} - \mathbf{b}) \quad . \quad (2)$$

A. Modeling the Topological Junction

Every purely topological junction is a linear reciprocal connection network [6]. It follows that we can collect q independent port voltages with $1 \leq q < N$ in a column vector \mathbf{v}_t , $p = N - q$ independent port currents in a column vector \mathbf{i}_t and find a pair of matrices \mathbf{Q} and \mathbf{B} of sizes $q \times N$ and $p \times N$ such that [27]

$$\mathbf{v} = \mathbf{Q}^T \mathbf{v}_t \quad , \quad \mathbf{i} = \mathbf{B}^T \mathbf{i}_t \quad (3)$$

and $\mathbf{Q}^T \mathbf{B} = \mathbf{0}$, where $\mathbf{0}$ is a properly sized matrix of zeros. In the WD domain the topological junction is characterized by a $N \times N$ scattering matrix that relates vectors of waves as

$$\mathbf{a} = \mathbf{S}\mathbf{b} \quad , \quad (4)$$

where \mathbf{S} can be computed with one of the following two dual formulas [6]

$$\mathbf{S} = 2\mathbf{Q}^T(\mathbf{Q}\mathbf{Z}^{-1}\mathbf{Q}^T)^{-1}\mathbf{Q}\mathbf{Z}^{-1} - \mathbf{I} \quad , \quad (5)$$

$$\mathbf{S} = \mathbf{I} - 2\mathbf{Z}\mathbf{B}^T(\mathbf{B}\mathbf{Z}\mathbf{B}^T)^{-1}\mathbf{B} \quad , \quad (6)$$

where \mathbf{I} is the $N \times N$ identity matrix.

B. Modeling Linear Elements

A large class of linear one-ports, including resistors, resistive sources, and inductors or capacitors whose dynamic equations are discretized using implicit linear multi-step discretization methods, e.g., trapezoidal method or backward differentiation methods, are characterized by the following Thévenin model in the discrete-time Kirchhoff domain [26]

$$v[k] = R_g[k]i[k] + V_g[k] \quad (7)$$

where k is the sampling index, $v[k]$ is the port voltage, $i[k]$ is the port current, $R_g[k]$ is a resistive parameter and $V_g[k]$ is a voltage parameter. According to (2), the same generic one-port is characterized by the following WD scattering relation

$$b[k] = \left(\frac{R_g[k] - Z[k]}{R_g[k] + Z[k]} \right) a[k] + \left(\frac{2Z[k]}{R_g[k] + Z[k]} \right) V_g[k] \quad . \quad (8)$$

It is always possible to *adapt* a WD linear element of this kind (which means, to eliminate the instantaneous dependency between $b[k]$ and $a[k]$) by setting $Z[k] = R_g[k]$ in such a way that (8) reduces to $b[k] = V_g[k]$ [26].

C. Modeling Nonlinear Elements

In contrast to the linear elements mentioned in the previous subsection, nonlinear one-ports cannot be adapted. As an example of the sort, let us consider a diode characterized by the following *extended Shockley diode model* [25]

$$f(v, i) = I_s \left(\exp\left(\frac{v - R_s i}{\eta V_t}\right) - 1 \right) + \frac{v - R_s i}{R_p} - i = 0 \quad (9)$$

where the sampling index k is omitted for the sake of brevity, I_s is the saturation current, η is the ideality factor, V_t is the thermal voltage, while R_s and R_p are the series resistance and the shunt resistance of the p-n junction, respectively. Such an element cannot be adapted, since, upon substitution (2), equation (9) cannot be written in the form (8) because a Thévenin representation of the diode at a fixed time instant would require parameters R_g and V_g to depend on the considered operating point. If we consider a generic operating point $\{v_o, i_o\}$ on the nonlinear curve $f(v, i)$ we can locally describe the diode behavior by performing a linearization in the form

$$v = R_g(v_o, i_o) i + V_g(v_o, i_o) \quad (10)$$

where

$$R_g(v, i) = - \frac{\partial f(v, i) / \partial i}{\partial f(v, i) / \partial v} = \frac{1 + \frac{R_s}{R_p} + \frac{I_s R_s}{\eta V_t} \exp\left(\frac{v - R_s i}{\eta V_t}\right)}{\frac{1}{R_p} + \frac{I_s}{\eta V_t} \exp\left(\frac{v - R_s i}{\eta V_t}\right)} \quad , \quad (11)$$

$$V_g(v, i) = v - R_g(v, i) i \quad . \quad (12)$$

Moreover, the computation of the reflected wave b given the incident wave a and the free parameter Z is not as simple as in the linear case; the method based on a scalar Newton-Raphson (NR) solver discussed in [25] and [26] is used for this purpose.

D. Scattering Iterative Method

The SIM was formalized in [23], [24] for the solution of large static nonlinear photovoltaic arrays and generalized in [25], [26] for the solution of dynamic nonlinear audio circuits. The algorithm, here restated, is composed of the following four stages performed at each sampling step k .

1) *Initialization, Update of \mathbf{Z} and \mathbf{S}* : The free parameters $Z_1[k], \dots, Z_N[k]$ (diagonal entries of \mathbf{Z}) are set as close as possible to the slope of the tangent line passing through the operating point of the $v-i$ curve. For linear elements the optimal values can be set a-priori as $Z_n[k] = R_{gn}[k]$, where the subscript n refers to the n th port. For nonlinear elements slopes can only be estimated, hence we set $Z_j[k] = R_{gj}(v_j[k-1], i_j[k-1])$ with $1 \leq j \leq J$. The scattering matrix $\mathbf{S}[k]$ is computed using the updated $\mathbf{Z}[k]$ matrix, according to (5) or (6). As initial guesses of the iterative fixed-point method we set $\mathbf{a}^{(0)}[k] = \mathbf{a}^{(0)}[k-1]$ and $\mathbf{v}^{(0)}[k] = \mathbf{v}^{(0)}[k-1]$.

2) *Local Scattering Stage*: Waves reflected from adapted linear elements are computed as $b_n[k] = V_{gn}[k]$. Values of waves reflected from nonlinear elements are found using a fixed-point technique according to

$$b_n^{(\gamma)}[k] = 2v_n^{(\gamma)}[k] - a_n^{(\gamma-1)}[k] \quad (13)$$

where $\gamma > 0$ is the SIM iteration index, $v_n^{(\gamma)}$ is computed by a scalar implicit or explicit nonlinear equation solver, like the NR solver used for diodes.

3) *Global Scattering Stage*: At the γ th iteration, the waves reflected by the WD junction are computed as

$$\mathbf{a}^{(\gamma)}[k] = \mathbf{S}[k]\mathbf{b}^{(\gamma)}[k] \quad (14)$$

4) *Convergence Check*: Local and global scattering stages are iteratively repeated until the following condition is met

$$\|\mathbf{v}^{(\gamma)}[k] - \mathbf{v}^{(\gamma-1)}[k]\|_2 < \epsilon_{\text{SIM}} \quad (15)$$

where ϵ_{SIM} is a small tolerance, e.g., $\epsilon_{\text{SIM}} = 10^{-3}$.

III. STANDARD SIM PERFORMANCE ANALYSIS

We define some quantitative measures that are used for the evaluation of SIM in terms of efficiency and percentage of computational load required by each stage of the algorithm. Such an analysis is useful to identify the most computationally demanding operations of SIM and to find strategies for minimizing their execution time. The considered measures are the following.

1) *Real Time Ratio (RTR)*: RTR already discussed in [25] is a dimensionless quantity indicating how fast the simulation is with respect to real time. If we consider an input signal of X samples and t_c the time needed by the algorithm to process them, the RTR can be computed as $\text{RTR} = (t_c \cdot F_s)/X$, where F_s is the sampling frequency. The algorithm can run in real time only if $\text{RTR} < 1$.

2) *Number of SIM Iterations*: average number of iterations per sample needed to reach convergence.

3) *Iteration Time*: average time per sample spent in the iterative process, composed of local scattering stage, global scattering stage and convergence check.

4) *\mathbf{Z} and \mathbf{S} Update Time*: average time per sample needed to update the port resistances Z_j and recompute the scattering matrix \mathbf{S} .

A. Example of Application

As an example of application, we implement the circuit of the asymmetric diode clipper in Fig. 1 used in distortion pedals for electric guitar or bass. The circuit parameters of the linear elements are $R_{\text{in}} = 10 \text{ k}\Omega$ and $C = 1 \text{ nF}$. Parameters of diodes D_c , D_d , D_f and D_g are: $I_s = 1 \text{ pA}$, $\eta = 2.19$, $V_{\text{th}} = 26 \text{ mV}$, $R_p = 10^7 \Omega$ and $R_s = 10^{-2} \Omega$. Diode D_e shares the same values of parameters of the rest of diodes, except for $I_s = 0.1 \text{ pA}$ and $\eta = 1.94$. The reference circuit in Fig. 1 is implemented in the WD domain using the trapezoidal rule for discretizing the time-derivative of the capacitor as in traditional WDFs [3], [26] and the resulting WD structure is shown in Fig. 2. The WD topological junction is characterized by the following fundamental loop matrix [6]

$$\mathbf{B} = \begin{bmatrix} 1 & 0 & 0 & 1 & 0 & 0 & 0 \\ 0 & 1 & 1 & 0 & 1 & 0 & 0 \\ -1 & -1 & -1 & 0 & 0 & 1 & 0 \\ -1 & -1 & -1 & 0 & 0 & 0 & 1 \end{bmatrix} \quad (16)$$

that allows us to compute the WD scattering matrix with (6). The circuit is emulated in the WD domain using SIM in the MATLAB environment. The input signal V_{in} is an A4 (440 Hz) lasting four seconds played with an electric guitar, recorded at a sampling frequency $F_s = 44.1 \text{ kHz}$ and then upsampled by a factor of 4 to avoid aliasing due to the nonlinear processing. The column named STD-SIM in Table I shows the values of all the measures discussed in this Section referred to the

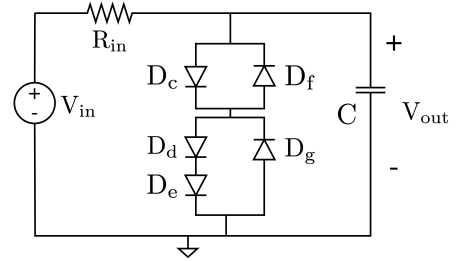


Fig. 1. Asymmetric diode clipper circuit.

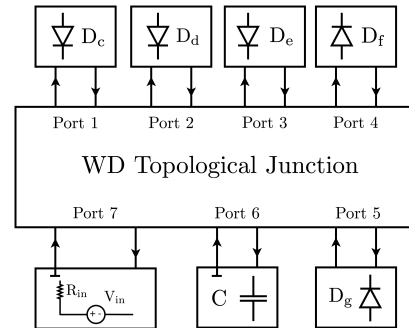


Fig. 2. WD structure corresponding to the circuit in Fig. 1.

TABLE I
PERFORMANCE COMPARISON BETWEEN STD-SIM AND DSR-SIM

	STD-SIM	DSR-SIM
RTR	1.43	0.89
Avg. Numb. of Iterations per Sample	1.48	1.60
Avg. Iteration Time per Sample	2.25 μs	2.40 μs
Avg. Z, S Update Time per Sample	5.88 μs	2.66 μs
Avg. Total Time per Sample	8.13 μs	5.06 μs

TABLE II
PERCENTAGES OF EXECUTION TIME IN STD-SIM AND DSR-SIM

	STD-SIM	DSR-SIM
Iteration Time	27.7 %	47.4 %
Z, S Update Time	72.3 %	52.6 %

standard SIM. The algorithm does not run in real time as the RTR is greater than 1. A relevant aspect concerning the time needed for executing specific tasks of the algorithm is that most of the computational load is due to the update of \mathbf{Z} and the consequent formation of \mathbf{S} at each sampling step. This fact is confirmed by the column named STD-SIM of Table II that shows how higher is the percentage of time required to update \mathbf{S} (more than 70%) with respect to the percentage of time spent in the iterative process (local scattering stage, global scattering stage and convergence check) out of the total execution time.

IV. DYNAMIC SCATTERING MATRIX RECOMPUTATION

In the light of the performance analysis presented in the previous section, we deduce that the main bottleneck of SIM is the update of \mathbf{S} performed at every sample. In order to alleviate this problem we here propose a technique called *Dynamic Scattering matrix Recomputation* (DSR) that is aimed at updating the scattering matrix less frequently and in a smarter fashion. Keeping the free parameters Z_j as close as possible to the resistance parameter $R_{gj}(v_o, i_o)$ of the Thévenin representation of the diode at a specific operating point $\{v_o, i_o\}$ has been shown in [23], [25], [26] to have the advantage of maintaining the spectral radius of the iteration matrix of SIM small, granting a high speed of convergence of the fixed-point process [23]. However, the advantage gained in updating the free parameters Z_j is counterbalanced by the cost of reforming the scattering matrix \mathbf{S} ; therefore, the policy of performing the update at each sample might be suboptimal. For this reason, we propose to monitor the following quantity at the beginning of each sampling step k

$$\psi[k-1] = \sum_{j=1}^J |R_{gj}(v_j[k-1], i_j[k-1]) - Z_j[k-1]| \quad (17)$$

where $v_j[k-1]$ and $i_j[k-1]$ are the voltage across and the current through the element connected to port j at sampling step $k-1$, while $R_{gj}(v_j[k-1], i_j[k-1])$ is the resistive Thévenin parameter that in the case of diodes with extended Shockley model is computed using eq. (12). Defined a positive threshold ξ_{DSR} , if $\psi[k-1] \leq \xi_{\text{DSR}}$, then the free parameters Z_j are left unaltered, i.e., $Z_j[k] = Z_j[k-1]$ with $1 \leq j \leq J$; if,

instead, $\psi[k-1] > \xi_{\text{DSR}}$, then matrices \mathbf{Z} and \mathbf{S} are updated as in the standard SIM, i.e., $Z_j[k] = R_{gj}(v_j[k-1], i_j[k-1])$.

A. Example of Application: Real-Time MATLAB Implementation of the Asymmetric Diode Clipper

We implement in the MATLAB environment the same asymmetric diode clipper considered in the previous section using the DSR variant of SIM and setting $\xi_{\text{DSR}} = 1 \text{ k}\Omega$. Fig. 3 confirms that the accuracy of the WD implementation based on DSR-SIM is the same of an LTSpice simulation. Fig. 4 shows how the signal ψ (orange continuous line) varies over time, while compared with the input signal (blue dashed line). It is worth noticing that the signal ψ alternates portions in which it is almost constant to sudden variations and spikes. The spikes mainly occur in correspondence to zero crossings of the input signal V_{in} . This is due to the fact that polarity changes in the input signal induce some diodes to switch from forward bias mode to reverse bias mode and vice-versa, causing significant variations of the resistive Thévenin parameters $R_{gj}(v_j, i_j)$. The DSR-SIM column of Table I reports the values of all the performance measures discussed in Section III. We notice

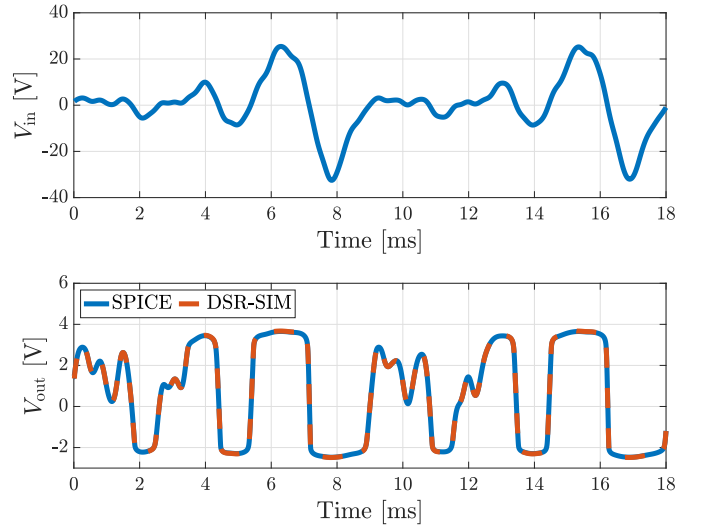


Fig. 3. Asymmetric diode clipper. V_{in} signal (upper plot). V_{out} signal: comparison between SPICE and WDF based on DSR-SIM (lower plot).

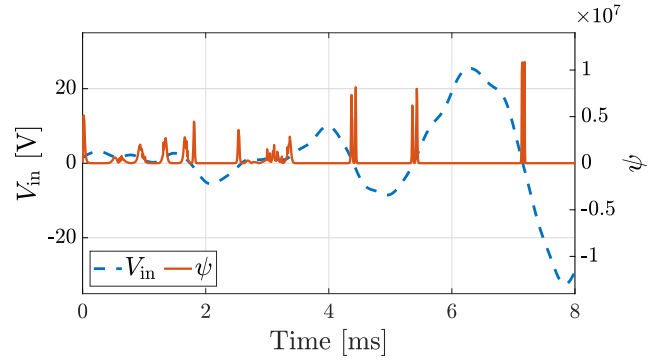


Fig. 4. Asymmetric diode clipper. WDF based on DSR-SIM: signal ψ synchronized with the input signal V_{in} .

TABLE III
CPU USAGE COMPARISON BETWEEN STANDARD SIM AND DSR-SIM

	STD-SIM	DSR-SIM
CPU % (4×)	3.5%	2.4%
CPU % (8×)	6.1%	4.6%

that the WD implementation based on DSR-SIM can now run in real-time in MATLAB because $RTR < 1$, unlike the implementation with STD-SIM which is almost 1.6 times slower. Table II instead, shows how much more balanced the iteration time and the update time are in the DSR-SIM case than in the STD-SIM case.

V. C++ AUDIO PLUGIN RUNNING IN REAL-TIME

In order to further verify the effectiveness of the proposed approach, we developed an audio plugin that wraps the virtual analog simulation of the asymmetric diode clipper. We used C++ in the scope of the JUCE framework, as done for the development of various plugins available on the market. We compiled our code as an Audio Unit (AU) plugin, and we tested it in the REAPER software with different guitar tracks. Optimizing the code in C++ we managed to implement the reference circuit in the WD domain both using STD-SIM and DSR-SIM. However, as reported in Table III, the average CPU usage is noticeably reduced when the DSR procedure is enabled. At 4× oversampling the plugin uses $\simeq 30\%$ less CPU time, while at 8× the performance gain is $\simeq 25\%$. Our audio plugin runs in real-time in every tested scenario, on a laptop with a dual-core Intel i5 processor.

VI. CONCLUSION

In this paper, an in-depth analysis of the computational requirements of SIM has been presented and the Dynamic Scattering Matrix Recomputation (DSR) technique has been proposed for improving its performance. The DSR technique significantly reduces the computational cost of SIM-based Virtual Analog implementations in the WD domain, without sacrificing accuracy. As an example of application that proves the effectiveness of the proposed method, an audio plugin, that implements an asymmetric diode clipper with five separated diodes in real-time, has been developed.

REFERENCES

- [1] G. De Sanctis and A. Sarti, "Virtual analog modeling in the wave-digital domain," *IEEE Trans. Audio, Speech, Language Process.*, vol. 18, pp. 715–727, May 2010.
- [2] A. Bernardini and A. Sarti, "Towards inverse virtual analog modeling," in *Proc. 22nd Int. Conf. Digital Audio Effects*, Birmingham, UK, Sept. 2–6 2019.
- [3] A. Fettweis, "Wave digital filters: Theory and practice," *Proc. IEEE*, vol. 74, no. 2, pp. 270–327, Feb. 1986.
- [4] D. Fränken, J. Ochs, and K. Ochs, "Generation of wave digital structures for networks containing multiport elements," *IEEE Trans. Circuits Syst. I: Regular Papers*, vol. 52, no. 3, pp. 586–596, March 2005.
- [5] K. J. Werner, A. Bernardini, J. O. Smith, and A. Sarti, "Modeling circuits with arbitrary topologies and active linear multiports using wave digital filters," *IEEE Transactions on Circuits and Systems I: Regular Papers*, vol. 65, no. 12, pp. 4233–4246, Dec. 2018.

- [6] A. Bernardini, K. J. Werner, J. O. Smith, and A. Sarti, "Generalized wave digital filter realizations of arbitrary reciprocal connection networks," *IEEE Transactions on Circuits and Systems I: Regular Papers*, vol. 66, no. 2, pp. 694–707, Feb. 2019.
- [7] K. J. Werner, W. R. Dunkel, M. Rest, M. J. Olsen, and J. O. Smith III, "Wave digital filter modeling of circuits with operational amplifiers," in *Proc. Eur. Signal Process. Conf.*, Budapest, Hungary, Aug. 2016, pp. 1033–1037.
- [8] M. Verasani, A. Bernardini, and A. Sarti, "Modeling Sallen-Key audio filters in the wave digital domain," in *2017 IEEE International Conference on Acoustics, Speech and Signal Processing (ICASSP)*, March 2017, pp. 431–435.
- [9] K. Meerkötter and R. Scholz, "Digital simulation of nonlinear circuits by wave digital filter principles," in *IEEE Int. Symp. Circuits Syst.*, May 8–11 1989, pp. 720–723.
- [10] A. Sarti and G. De Sanctis, "Systematic methods for the implementation of nonlinear wave-digital structures," *IEEE Trans. Circuits Syst. I, Reg. Papers*, vol. 56, pp. 460–472, Feb. 2009.
- [11] A. Bernardini, K. J. Werner, A. Sarti, and J. O. Smith, "Modeling a class of multi-port nonlinearities in wave digital structures," in *Proc. 23rd European Signal Processing Conference (EUSIPCO)*, Nice, France, Aug. 31 – Sept. 4 2015, pp. 669–673.
- [12] A. Bernardini and A. Sarti, "Dynamic adaptation of instantaneous nonlinear bipoles in wave digital networks," in *Proc. 24th European Signal Processing Conference (EUSIPCO)*, Budapest, Hungary, Aug. 29 – Sept. 2 2016, pp. 1038–1042.
- [13] A. Bernardini, K. J. Werner, A. Sarti, and J. O. Smith III, "Modeling nonlinear wave digital elements using the Lambert function," *IEEE Transactions on Circuits and Systems I: Regular Papers*, vol. 63, no. 8, pp. 1231–1242, Aug. 2016.
- [14] A. Bernardini and A. Sarti, "Canonical piecewise-linear representation of curves in the wave digital domain," in *Proc. 25th European Signal Processing Conference (EUSIPCO)*, Aug 2017, pp. 1125–1129.
- [15] A. Bernardini, A. E. Vergani, and A. Sarti, "Wave digital modeling of nonlinear 3-terminal devices for virtual analog applications," *Circuits, Systems, and Signal Processing*, vol. 39, pp. 3289–3319, Jan. 2020.
- [16] A. Bernardini and A. Sarti, "Biparametric wave digital filters," *IEEE Transactions on Circuits and Systems I: Regular Papers*, vol. 64, no. 7, pp. 1826–1838, July 2017.
- [17] C. W. Ho, A. E. Ruehli, and P. A. Brennan, "The modified nodal approach to network analysis," *IEEE Trans. Circuits Syst.*, vol. 22, no. 6, pp. 504–509, June 1975.
- [18] M. Holters and U. Zölzer, "Physical modeling of a wah-wah effect pedal as a case study for application of the nodal dk method to circuits with variable parts," in *Proc. 14th Conf. Digital Audio Effects*, Paris, France, Sept. 19–23 2011.
- [19] A. Falaize and T. Hélie, "Passive guaranteed simulation of analog audio circuits: A port-Hamiltonian approach," *Applied Sciences*, vol. 6, no. 10, 2016.
- [20] M. J. Olsen, K. J. Werner, and J. O. Smith III, "Resolving grouped nonlinearities in wave digital filters using iterative techniques," in *Proc. 19th Int. Conf. Digital Audio Effects*, Brno, Czech Republic, Sept. 2016, pp. 279–286.
- [21] T. Schwerdtfeger and A. Kummert, "A multidimensional approach to wave digital filters with multiple nonlinearities," in *22nd Proc. European Signal Process. Conf.*, Lisbon, Portugal, Sept. 1–5 2014, pp. 2405–2409.
- [22] T. Schwerdtfeger and A. Kummert, "Nonlinear circuit simulation by means of Alfred Fettweis' wave digital principles," *IEEE Circuits and Systems Magazine*, vol. 19, no. 1, pp. 55–C3, Firstquarter 2019.
- [23] A. Bernardini, P. Maffezzoni, L. Daniel, and A. Sarti, "Wave-based analysis of large nonlinear photovoltaic arrays," *IEEE Trans. Circuits Syst. I, Reg. Papers*, vol. 65, no. 4, pp. 1363–1376, Apr. 2018.
- [24] A. Bernardini, A. Sarti, P. Maffezzoni, and L. Daniel, "Wave digital-based variability analysis of electrical mismatch in photovoltaic arrays," in *Proc. IEEE Int. Symp. Circuits Syst. (ISCAS)*, May 2018, pp. 1–5.
- [25] A. Bernardini, K. J. Werner, P. Maffezzoni, and A. Sarti, "Wave digital modeling of the diode-based ring modulator," in *Proc. 144th Audio Eng. Soc. Com.*, Milan, Italy, May 24–26 2018, conv. paper #10015.
- [26] A. Bernardini, P. Maffezzoni, and A. Sarti, "Linear multistep discretization methods with variable step-size in nonlinear wave digital structures for virtual analog modeling," *IEEE/ACM Transactions on Audio, Speech, and Language Processing*, vol. 27, no. 11, pp. 1763–1776, Nov. 2019.
- [27] S. Seshu and M. B. Reed, *Linear graphs and electrical networks*, 1st ed. AddisonWesley Publishing Company, Inc., Reading, MA, 1961.